The 4th European sCO_2 Conference for Energy Systems
March 23-24, 2021, Online Conference

2021-sCO2.eu-119

EVALUATION OF DETERIORATION IN VERTICAL SCO2 COOLING HEAT TRANSFER IN 3 MM TUBE

Andreas Wahl*
Institute of Nuclear Technology and Energy Systems (IKE), Stuttgart, Germany
andreas.wahl@ike.uni-stuttgart.de

Rainer Mertz
Institute of Nuclear Technology and Energy Systems (IKE), Stuttgart, Germany

Eckard Laurien
Institute of Nuclear Technology and Energy Systems (IKE), Stuttgart, Germany

Jörg Starflinger
Institute of Nuclear Technology and Energy Systems (IKE), Stuttgart, Germany

ABSTRACT

In the frame of EU-project sCO_2-flex the design of a 25 MWe supercritical CO_2 (sCO_2) Brayton cycle will be designed. The system will be optimized to meet flexibility requirements, while reducing environmental impact and focusing on cost efficiency. In the context of a sCO_2 Brayton cycle, the gas cooler is a key component to achieve a high overall efficiency. Close to the critical point, due to varying properties, heat transfer and pressure drop of carbon dioxide (CO_2) are difficult to predict. In case of vertical flow, acceleration and buoyancy effects induced by strong density gradients can cause a significant deterioration of the heat transfer.

In this publication, the cooling heat transfer coefficient (htc) is investigated in a 3 mm diameter tube with vertical flow orientation. Commonly used calculation methods of the heat transfer coefficient are presented. Although developed for heating of sCO_2, the mixed convection criterion of Jackson and Hall [7] is used to evaluate the heat transfer deterioration. The effects of the CO_2 mass flux of $141 - 354\ kg/m^2s$ and bulk fluid temperatures of $20 - 50\ °C$ with a constant pressure of $80\ bar$ on the heat transfer were examined. The transition between forced and mixed convection can be explained by the htc -values. The upwards flow shows a steady decrease in the htc with the reduction of the mass flux. However, the downwards flow shows significant effects of buoyancy. At low mass flux the distinct peak in the htc at the pseudocritical temperature (T_{pc}) disappears.

INTRODUCTION

A sCO_2 Brayton cycle offers a number of benefits over competing power plant cycles. A high plant efficiency can be achieved due to the favourable fluid properties in the supercritical region. This is resulting in increased electricity production with the same fuel consumption [16]. The high density of sCO_2 allows to reduce the necessary compressor work and leads to a reduction in the overall size of the power plant [4]. The reduced size of turbomachinery, boiler and heat exchangers can be further translated into reduced capital costs.The moderate value of its critical pressure ($7.38\ MPa$) makes CO_2 more economical than water where the critical point is much higher ($22.1\ MPa$). A low heat rejection temperature leads to power cycles with high efficiencies. The critical temperature of CO_2 ($31°C$) contributes to that, however, it is not too low, to be cooled by the ambient temperature. CO_2 is a non-toxic and non-flammable natural working fluid with ODP = 1 (ozone depletion potential) and GWP = 1 (global warming potential). It is available in sufficient quantities at reasonable costs. In environmental, cost and safety terms, CO_2 is regarded as an ideal natural refrigerant [19].

The properties of sCO_2 (Figure 1) lead to significant differences in the heat transfer characteristics. This is caused by rapid changes of thermo physical properties close to the critical point. The thermophysical properties are derived by the NIST/REFPROP database [5]. Thus, specific equation of state [11] and transport equations [6, 23] were used.

The understanding of heat transfer enhancement and deterioration phenomena during cooling in a small diameter tube is crucial to develop new concept of compact heat exchanger for the Brayton cycle, able to work with high efficiency, speed and reliability under high CO_2 pressure and low pinch point. The thermo physical properties change strongly with temperature and pressure. As shown in Figure 1, the viscosity (η) and density (ρ) are strongly decreasing with increasing temperature. The

* corresponding author(s)

DOI: 10.17185/duepublico/73957

isobaric heat capacity (c_p) and thermal conductivity (λ) pass through a peak crossing the pseudocritical temperature.

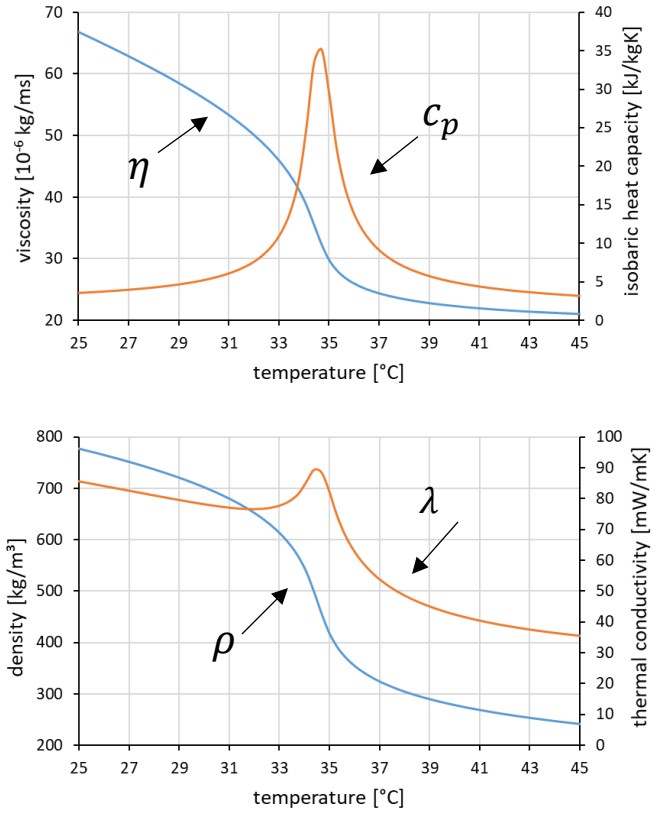

Figure 1: properties of CO2 at 80bar

In this study, the heat transfer under cooling conditions was determined at different mass fluxes, temperatures and flow orientations. The effects of the parameters on the heat transfer were demonstrated.

STATE OF THE ART OF HEAT TRANSFER DURING COOLING

A number of researchers have experimentally investigated the cooling heat transfer and pressure drop performance of CO_2 in tubes of different sizes. The research has been concentrated on tubes ranging from 0.5 to 10.7 mm in horizontal flow [3, 10, 13, 14, 17, 18, 21, 25]. Limited research is available for cooling heat transfer in vertical flow orientation. Jiang et al. [8] investigated the heat transfer during cooling in a 2 mm diameter tube with a combination of experimental measurements and numerical simulations. The results show that the local heat transfer coefficients vary significantly along the tube for different flow orientations. Bruch [2] investigated experimentally the cooling heat transfer of sCO_2 in a copper tube with an inner diameter of 6 mm. The test section consists of two vertical tube-in-tube heat exchangers connected in series by means of a U-bend. In the experiment, the in- and outlet temperature of CO_2 and cooling media was measured and treated with an integral method to determine the heat transfer coefficient.

The method to approach the deteriorated heat transfer of supercritical fluids in general and supercritical CO_2 in specific was developed in the heating case. The research on sCO_2 heating in direct electrical heated tubes lead to the development of criterions for the deterioration of heat transfer in vertical flow. Different criterions can be found in literature which are either based on the effect of flow acceleration or on the effect of buoyancy [7, 15, 20]. The experiments conducted with circular tubes of different diameters work on validation and improvement of the criterions and equations [9, 12, 13]. Currently and ongoing experiments at IKE with a 4 mm and 8 mm tube will contribute to this field of research [22]. Bruch [2] is the only author who applied a deterioration criterion to the cooling heat transfer. The semi-empirical parameter ($Gr/Re^{2.7}$) by Jackson and Hall [7] was applied to characterize the influence of natural convection on turbulent vertical flow. Fundamentally, mixed convection can be described with the Richardson-number, which compares buoyancy forces and the inertial forces. The Richardson number Ri is defined as a ratio of the Grashof number Gr and the Reynolds number Re to the square:

$$Ri = \frac{Gr}{Re^2} \tag{1}$$

Using the parameter, mixed convection has a significant influence on the heat transfer when:

$$\frac{Gr}{Re^{2.7}} > 10^{-5} \tag{2}$$

The Grashof number Gr used by Jackson and Hall [7] is calculated with the difference between bulk density ρ_b and the average density $\bar{\rho}$:

$$Gr = \frac{(\rho_b - \bar{\rho}) \cdot \rho_b \cdot g \cdot d^3}{\eta_b^2} \tag{3}$$

The average density $\bar{\rho}$ is calculated with the approximation by Bae and Yoo [1]:

$$\bar{\rho} \approx \begin{cases} \dfrac{(\rho_w + \rho_b)}{2} \; for\; T_w > T_{pc}\; or\; T_b < T_{pc} \\ \dfrac{[\rho_b(T_b - T_{pc}) + \rho_w(T_{pc} - T_w)]}{T_b - T_w} \; for\; T_w < T_{pc} < T_b \end{cases} \tag{4}$$

The selected pure forced convection correlation of Bruch [2] is the one by Jackson and Hall [7]:

$$\mathrm{Nu_{FC}} = 0.0183 Re_b^{0.82} \overline{Pr}_b^{0.5} \left(\frac{\rho_b}{\rho_w}\right)^{-0.3} \tag{5}$$

The results of the experimental investigation were plotted in dimensionless form (Figure 2). The resulting functions of the downwards stream are the following:

$$\frac{Gr}{Re^{2.7}} < 4.2 \cdot 10^{-5}: \quad \frac{Nu_b}{Nu_{FC}} = 1 - 75\left(\frac{Gr}{Re^{2.7}}\right)^{0.46} \tag{6}$$

$$\frac{Gr}{Re^{2.7}} > 4.2 \cdot 10^{-5}: \quad \frac{Nu_b}{Nu_{FC}} = 13.5\left(\frac{Gr}{Re^{2.7}}\right)^{0.40} \tag{7}$$

The region of forced convection is present at $Gr/Re^{2.7} < 10^{-6}$ with only little difference to unity. With increasing mixed convection parameter, the heat tranfser deteriorates strongly. The strongest deterioration is present in the mixed convection area. With further increase of the mixed convection factor, the flow regime converts to free convection. The heat transfer recovers in this area.

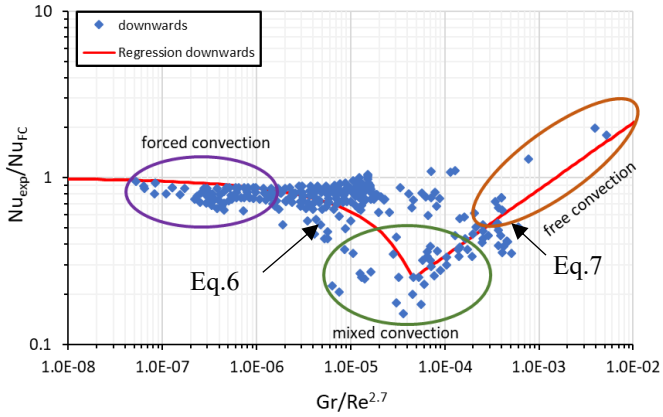

Figure 2: Evolution of Nusselt number with the mixed convection parameter by Bruch [15]

EXPERIMENTAL SET-UP

The SCARLETT test loop provides sCO2 under defined boundary conditions. Figure 3 illustrates of the SCARLETT test loop, which is described as follows [24].

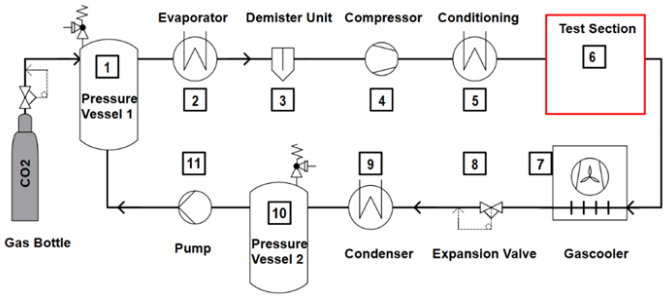

Figure 3: P&I diagramm of the SCARLETT test loop

After evacuating the loop with a vacuum pump, the pressure vessels (1, 10) are filled with CO_2 by a gas bottle. During normal operation, liquid CO_2 flows from the pressure vessel 1 through an electrical heated evaporator (2) and is slightly superheated. After leaving a demister unit (3), where remaining liquid CO_2 is separated from the flow, it enters a compressor (4), where it is compressed to a certain pressure and simultaneously heated by the compression.

Before entering a test section, there is a conditioning (5) of the sCO_2, which means that a defined temperature can be adjusted via cooling or heating the sCO_2 mass flow rate. In the test-section (6) different kind of experiments can be performed. After leaving the test section, the sCO_2 is cooled down in a gas cooler (7) followed by the expansion in an expansion valve (8). Before it enters the pressure vessel 2 (10) the CO_2 can be cooled down again in a condenser (9). Finally, it is pumped back from the pressure vessel 2 into the pressure vessel 1. The sCO_2 mass flow rate in the SCARLETT test loop can be adjusted from about 30 to 110 g/s. Lower mass flow rate in the test section can be achieved by bypassing with needle valves. It must be mentioned, that the achievable mass flow rate depends on the compressor performance map, which leads to less mass flow rate at higher pressures and vice versa. The sCO_2 temperature at the inlet of the test section can be varied from about 0 to 140 °C and the pressure up to 110 bar.

The test section applied in this report consists of a stainless steel tube with 1000 mm length. The inner diameter is 3 mm and the outer tube diameter is 5 mm. The experimentally cooled length of the tube is 500 mm. The annulus were designed to lead the thermocouples to the inner tube, deliver the cooling media in- and outflow, and close the annulus stream leak-tight. The flanges center the tube in the annulus. The differential pressure was measured by drilling holes into the tube wall. With 100 mm of adiabatic length at both sides of the tube, the differential pressure was measured at a length of 700 mm (Figure 4). The accuracy of the pressure transducer was 0.15 % of full range of 1/100 bar.

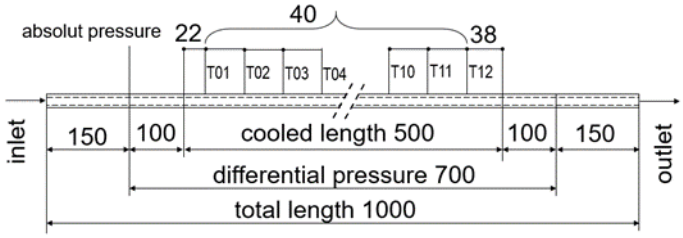

Figure 4: Detailed view of the test tube (All dim. in mm)

T-type thermocouples are soldered into milled channels on the surface of the tube (Figure 5). Before the installation, the thermocouples were calibrated within a range of 5-60 °C by the use of a high accurate reference resistance temperature detector (RTD, calibrated to 0.02 K). The resulting accuracy of the T-type thermocouples was ±0.1 K. The thermocouples are coated with stainless steel leading to high durability against corrosion.

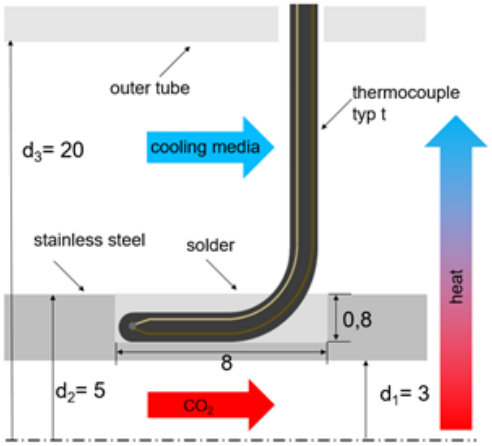

Figure 5: Detailed view of the thermocouple soldering in the tube surface (All dim. in mm)

The heat conductance in the thermocouple wire could lead to a measurement error, thus the thermocouples have to be embedded a certain length inside the tube to eliminate this influence. The T-type thermocouples have a diameter of 0.5 mm. They are bended and laid in the milled channels (0.8x0.8x8mm depth/ width/length). Additional to the measurement errors, the error of the manual soldering process has to be considered. For example, the manufacturing inaccuracies of the milled channels, the placing in the channel to the assumed accuracy of the wall temperature of the stainless-steel tube of ±0.2 K. The bending of the thermocouple leads to an asymmetry of the temperature measurement points in the cooled length. The first measurement position (T_{01}) is at 22 mm of the cooled length. The spacing is equal along the tube with 40 mm between the measurement positions. The thermocouples were mounted in-line. The solder alloy used to connect the tube with the thermocouples was a 96 % tin and 4 % silver mixture with implemented colophony. This material has a low temperature melting point (Solidus: 221 °C, Liquidus 238 °C), which does not exceed the temperature range of T-type thermocouples (-40 °C…+350 °C) and leads to a good thermal connection of the two components due to the high thermal conductivity. The accuracy of the RTD's to measure both flows at in- and outlet were ±0.1 K. The accuracy of the Coriolis-type mass flow meter was assumed to be 0.3 %. All measurement quantities of the test section are displayed in Figure 6.

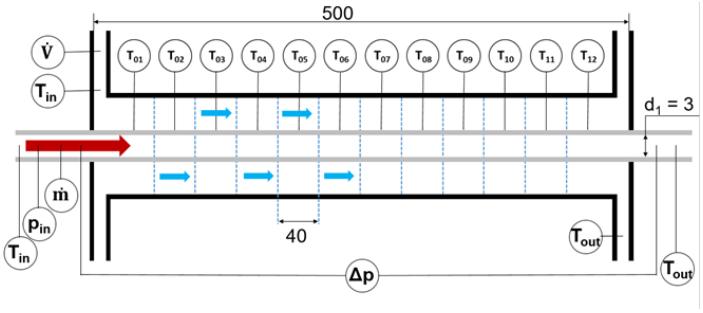

Figure 6: measured quantities in the experiment(All dim. in mm)

DATA REDUCTION

The removed heat can be calculated with the in- and outlet temperatures T_{in} T_{out}, inlet pressure p_{in} and differential pressure Δp of the CO_2 flow:

$$\dot{Q}_{CO2} = \dot{m}_{CO2} * [h_{in}(T_{in}, p_{in}) - h_{out}(T_{out}, p_{in} - \Delta p)] \quad (9)$$

The temperature difference in the cooling media flow between in and outlet is too small to apply a caloric determination. The heat flux is calculated as following:

$$\dot{q}_{CO2} = \frac{\dot{Q}_{CO2}}{\pi d L} \quad (10)$$

The CO_2 bulk temperature $T_{CO2,b}$ for each experiment is the average of in- and outlet.

$$T_{CO2,b} = \frac{T_{CO2,in} + T_{CO2,out}}{2} \quad (11)$$

The twelve tube temperature measurements are averaged:

$$T_t = \frac{\sum_{i=1}^{12} T_{t,i}}{12} \quad (12)$$

The heat conduction of the tube wall leads to a difference between the measured tube wall $T_{R,i}$ and the CO_2 wall temperature $T_{CO2,w}$. For this reason, the tube wall measurement is assumed to be central between inner and outer surface:

$$T_{CO2,w} = T_t + \dot{q}_{CO2} \cdot \frac{\ln(\frac{4\ mm}{3\ mm})}{2\pi L \lambda} \quad (13)$$

The heat transfer coefficient is defined as the ratio of heat flux and temperature difference between CO_2 bulk and wall:

$$htc_{CO2} = \frac{\dot{q}_{CO2}}{\Delta T} \quad (14)$$

Caused by the fact, that in the supercritical region c_p und htc can change strongly, it is important to evaluate different definitions of the temperature difference ΔT. One option, as considered by Yoon et al. [25], Son et al. [21] und Liu et al. [14], is to calculate the difference of both averaged values $T_{CO2,b}$ (Eq.11) and $T_{CO2,w}$(Eq.13):

$$\Delta T_{average} = T_{CO2,b} - T_{CO2,w} \quad (15)$$

A second approach is to calculate the logarithmic mean temperature difference (LMTD):

$$\Delta T_{LMTD} = \frac{(T_{in} - T_{CO2,w,1}) - (T_{out} - T_{CO2,w,12})}{\ln(\frac{T_{in} - T_{CO2,w,1}}{T_{out} - T_{CO2,w,12}})} \quad (16)$$

with the CO_2-wall temperature at the first and the last measurement $T_{CO2,w,1}$ / $T_{CO2,w,12}$ as applied by Liao [13] and Dang [3]. The study aims to determine the htc as a local set of values. However, the changing thermophysical properties along the tube influence the heat transfer calculation. The LMTD method is based on the assumption of a constant property fluid. To limit the changes of the properties between the in- and outlet of CO_2, the temperature difference of the experiments was kept low if T_b is close to T_{pc}.

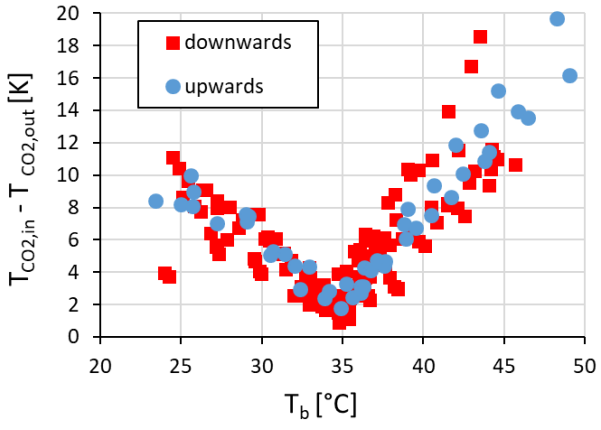

Figure 7: Temperature difference T_{in} - T_{out} over T_b

Higher temperature differences were only measured far away from T_{pc} (Figure 7). It results in a difference of both approaches of between +10% and -20% (Figure 8). In the vicinity of the pseudocritical temperature T_{pc}, htc_{ave} is up to 10% higher. Towards lower and higher temperatures, this tendency is reversed. In the liquid like region, the htc_{LMTD} is up to 10% higher and in the gas like region up to 20% higher. However, to ensure the accuracy of $\dot{q}_{CO2}$ determination, it is important to measure above a certain temperature difference between in-and outlet. This is due to the high c_p close to T_{pc}. To meet both requirements the temperature difference close to T_{pc} was kept around 2 K. The inaccuracies based on the measurements was kept below 20%. This assessment shows the good agreement of both approaches. However, only has little influence on the final evaluation of heat transfer deterioration which is based on a direct comparison of both flow direction. As from now, htc_{LMTD} is presented in reference to htc.

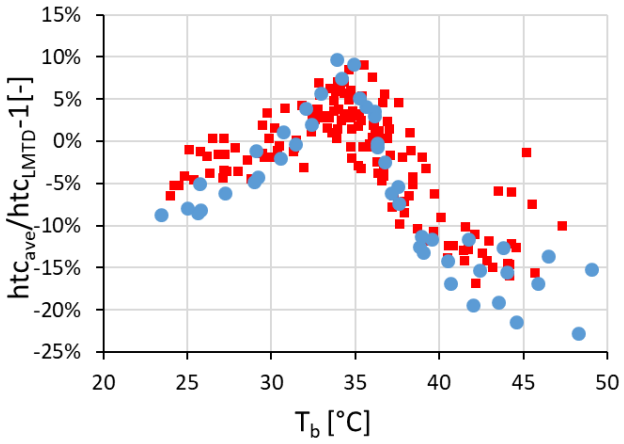

Figure 8: Difference of htc_{ave} / htc_{LMTD} over T_b

EXPERIMENTAL DATA

In this report, the experimental results of 204 experiments are presented. The parameter range is displayed in Table 1.

Table 1: Experimental parameter and number of experiments

CO_2		
temperature[°C]	pressure [bar]	mass flux [kg/m²s]
51-20	80	141-354

flow orientation ± 2°	
upwards	45
downwards	159

VERTICAL FLOW ORIENTATION

In the vertical upwards flow, free convection induces additional turbulence. The effective direction of forced convection is upwards while free convection is in downwards direction. The interaction of both effects leads to a parabolic velocity profile, which increases the velocity difference between the wall and the centreline and thus, increases the heat transfer.

From literature [2], it is known, that this influence is much smaller than in the downwards flow. In Figure 9, the htc-values for mass fluxes from 141 kg/m^2s to 283 kg/m^2s are shown. As expected, all three mass fluxes show a similar trend with a peak close to T_{pc}. It can be seen, that the enhancement of the mass flow leads to higher htc due to increases turbulent diffusion. Horizontal error bars represent temperature change from the inlet to the outlet of the test section, and vertical error bars represent the uncertainty in the measurement. Only two error bars are displayed with the aim to keep the diagram readable. The error bar shows what was mentioned previously, the temperature difference in the CO_2 flow is small to decrease the uncertainties in the heat transfer coefficient.

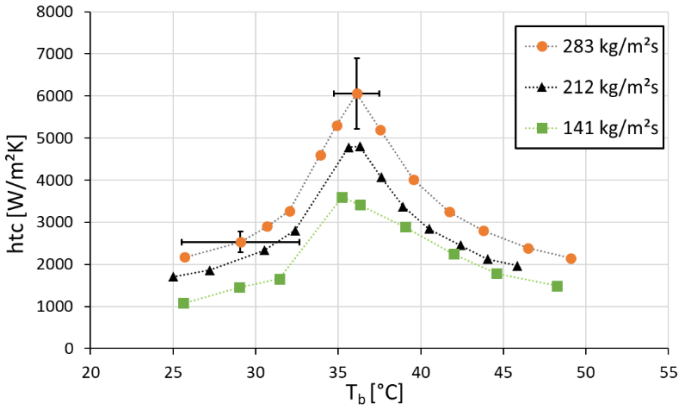

Figure 9: htc over T_b for different mass flux in vertical upwards flow

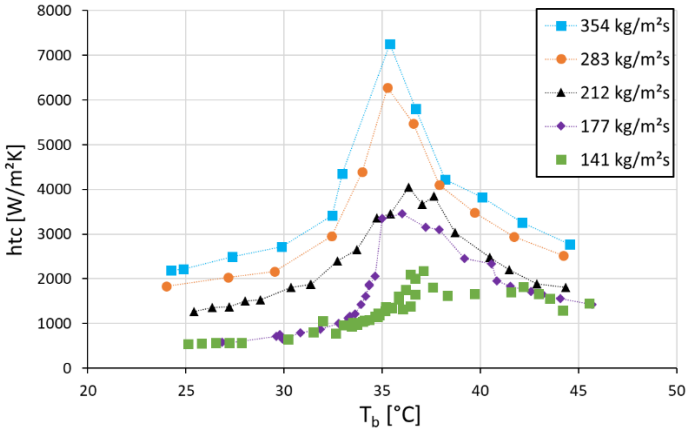

Figure 10: htc over T_b for different mass flux in vertical downwards flow

In the vertical downwards flow, the effective direction of both forced and free convection are in downwards direction. In this case, a m-shaped velocity profile develops. Due to this interaction, the velocity difference between wall and centreline is reduced, which can handicap the radial energy transfer. In the downwards flow, it is expected to see significant deterioration of the heat transfer, that means discrepancies to the forced convection regime. In Figure 10, the htc-values for mass fluxes from 141 kg/m^2s to 354 kg/m^2s in the vertical downwards flow are shown. With the reduction of the mass flux from 354 kg/m^2s to 283 kg/m^2s, a constant decrease of the htc-values can be seen. With further reduction of the mass flux, clear evidence of mixed convection is present. In the liquid like region ($T_b < 34.6°C$), the htc drops between 212 kg/m^2s and 177 kg/m^2s relatively strong. However, the htc remains constant with further reduction. At T_{pc}, a strong reduction of the htc can be seen at $G = 177\ kg/m^2s$. At this mass flux the abrupt change in the thermo physical properties seems to induce deterioration. The htc at $G = 141\ kg/m^2s$ shows a flat trend and thus, disagrees clearly from forced convection. In the temperature region $T_b < 33°C$ and $T_b > 42°C$, the htc is constant with further reduction from $G = 177\ kg/m^2s$ to 141 kg/m^2s .

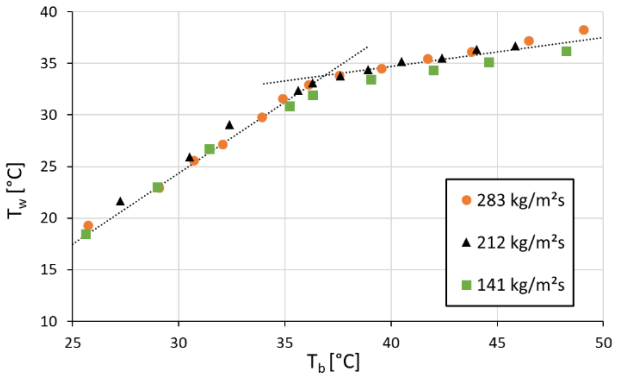

Figure 11: T_w over T_b for different mass flux in vertical upwards flow

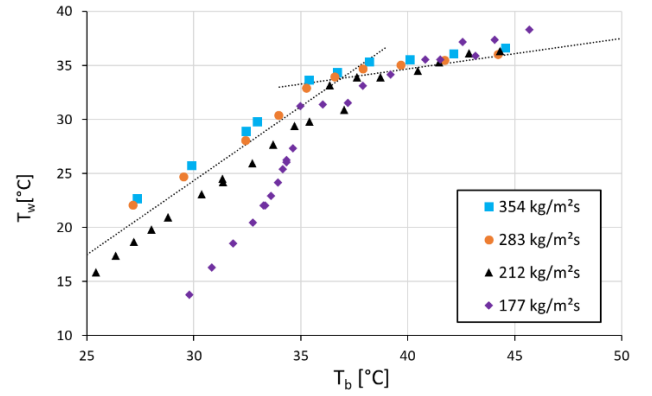

Figure 12: T_w over T_b for different mass flux in vertical downwards flow

In Figure 11 and Figure 12, the wall temperatures are presented as a function of the bulk temperature. In the upwards flow, the enhancement of the heat transfer with increasing mass flux leads to no difference in the wall temperature. The dotted lines visualize the tendencies. The differences between the gas and liquid-like region are significant. In the downwards flow, the heat transfer deterioration causes a strong decrease of the wall temperatures.

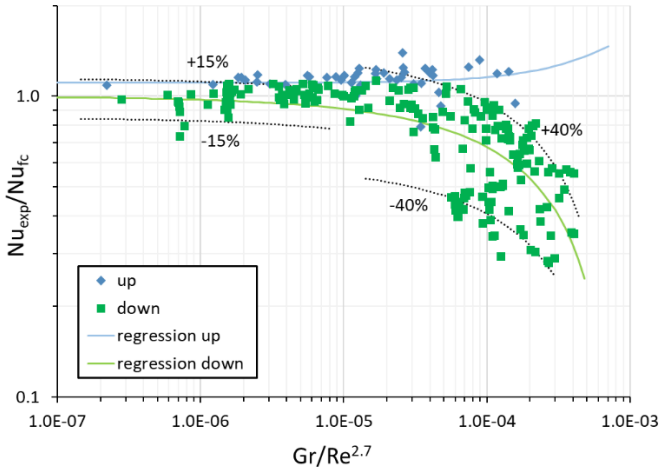

Figure 13: Evolution of ratio Nu_{exp}/Nu_{fc} with the mixed convection parameter $Gr/Re^{2.7}$ of the downwards and upwards flow

In Figure 13, results are presented in dimensionless form. For low values of the mixed convection parameter $Gr/Re^{2.7}$, forced convection is the predominant mechanism of heat transfer. The influence of free convection is negligible and the ratio Nu_{exp}/Nu_{fc} is close to unity for both flow directions. This also indicates a good agreement with the choosen forced convection equation by Dang [9]. As the parameter $Gr/Re^{2.7}$ increases, buoyancy forces are stronger and differences appear with flow direction. Heat transfer is enhanced in upwards flow and deteriorated in downwards flow. In the downwards flow a clear trend can be seen, however, the mean variation is relatively high. The transition to free convection, which is characterised with the recovery of the Nu_{exp}/Nu_{fc} ratio was not detected within the experimental boundary conditions. Equation 17 and 18 are the functions of the plotted regression of Figure 13.

upwards: $$\frac{Nu_b}{Nu_{fc}} = 1.107 + 510.2 * \frac{Gr}{Re^{2.7}} \quad (17)$$

downwards: $$\frac{Nu_b}{Nu_{fc}} = 1 - 46.4 * \left(\frac{Gr}{Re^{2.7}}\right)^{0.540} \quad (18)$$

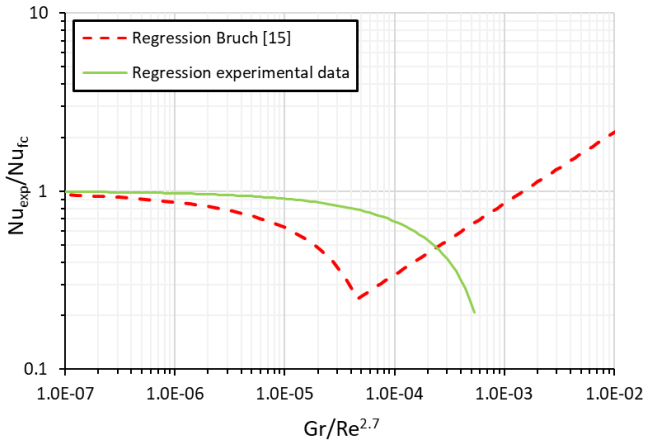

Figure 14: Comparison of proposed correlation of downwards flow with the correlation by Bruch [2]

Figure 14 compares the experimental regression (green) with the equation by Bruch [2]. The experiments show deterioration at higher $Gr/Re\hat{}2.7$ values. This might indicate, that the tube diameter is a relevant factor of the heat transfer deterioration in cooling heat transfer. It seems like that the phenomena of deterioration and recovery is shifted towards higher $Gr/Re^{2.7}$ values. The heat transfer recovery is expected to appear near the end of the plotted regression at $Gr/Re^{2.7} \approx 10^{-3}$. However, the experimental facility with its fixed cooling length would reduce the accuracy to an unacceptable level with further reduction of the mass flux.

CONCLUISON

At the IKE University Stuttgart, an experimental investigation was conducted to evaluate the heat transfer in a vertical cooled tube with 3 mm inner diameter. The results show an influence of mixed convection at a stepwise reduction of the mass flux. The transition from forced convection to mixed convection can be seen by means of the drop in the heat transfer coefficient. The analysis of the experimental data with the Jackson criterion resulted in a significant trend. However, the deterioration in downwards flow appeared at higher values of the criterion as detected by Bruch [15]. This comparison indicates that an influence on the diameter might be existing.

The findings of this report show, that in the design of the chiller for a supercritical CO_2 power cycle the flow direction could be an influencing factor. Usually, the CO_2 flows in horizontal tubes. The rotation speed of the fan controls the removed heat. If the vertical flow orientation is in consideration for such a heat exchanger, the designer should avoid the mixed convection flow area.

ACKNOWLEDGEMENT

This project has received funded by the European Union's Horizon 2020 research and innovation programme under grant agreement No 764690

NOMMENCLATUR

c_p	(J/kgK)	specific heat
d	(mm)	diamter
g	(m/s²)	acceleration of gravity
G	(kg/m²s)	mass flux
Gr	(-)	Grashof number
h	(kJ/kg)	specific Enthalpy
htc	(W/m²K)	heat transfer coefficient
L	(m)	length of discretization
$\dot{m}$	(kg/s)	mass flow rate
Nu	(-)	Nusselt number
p	(bar)	pressure
Pr	(-)	Prandtl number
Q	(W)	heat
$\dot{q}$	(W/m²)	heat flux
Re	(-)	Reynolds number
Ri	(-)	Richardson number
T	(°C)	temperature
V	(l/s)	volumetric flow

Greek symbols

Δp	(bar)	pressure drop
η	(kg/ms)	dynamic viscosity
λ	(W/mK)	heat conductivity
ρ	(kg/m³)	density

subscripts

b	bulk
CO_2	carbon dioxide
exp	experiment
fc	forced convection
in	inlet
LMTD	logarithmic mean temperature difference
out	outlet
pc	pseudo critical
t	tube
w	wall

REFERENCES

[1] Bae, J. H., Yoo, J. Y., and Choi, H. 2005. Direct numerical simulation of turbulent supercritical flows with heat transfer. J. Heat Transfer 17, 10, 105104.

[2] Bruch, A., Bontemps, A., and Colasson, S. 2009. Experimental investigation of heat transfer of supercritical carbon dioxide flowing in a cooled vertical tube. International Journal of Heat and Mass Transfer 52, 11-12, 2589–2598.

[3] Dang, C. and Hihara, E. 2004. In-tube cooling heat transfer of supercritical carbon dioxide. Part 1. Experimental measurement. International Journal of Refrigeration 27, 7, 736–747.

[4] Dostal, V., Driscoll, M. J., and Hejzlar, P. 2004. A Supercritical Carbon Dioxide Cycle for Next Generation Nuclear Reactors. MIT-ANP-TR-100.

[5] E. W. Lemmon, M. L. Huber, M. O. McLinden. 2010. REFPROP. Reference Fluid Thermodynamic and Transport Properties. NIST SRD 23, United States of America.

[6] Fenghour, A., Wakeham, W.A., Vesovic, V. 1998. The Viscosity of Carbon Dioxide.

[7] Jackson, J. D. and Hall, W. B. 1979. Forced Convection Heat Transfer to Fluids at Supercritical Pressure. Institution of Mechanical Engineers, Conference Publications 2.

[8] Jiang, P.-X., Zhao, C.-R., Shi, R.-F., Chen, Y., and Ambrosini, W. 2009. Experimental and numerical study of convection heat transfer of CO2 at super-critical pressures during cooling in small vertical tube. International Journal of Heat and Mass Transfer 52, 21-22, 4748–4756.

[9] Kim, D. E. and Kim, M.-H. 2011. Experimental investigation of heat transfer in vertical upward and downward supercritical CO2 flow in a circular tube. International Journal of Heat and Fluid Flow 32, 1, 176–191.

[10] Kondou, C. and Hrnjak, P. 2011. Heat rejection from R744 flow under uniform temperature cooling in a horizontal smooth tube around the critical point. International Journal of Refrigeration 34, 3, 719–731.

[11] Kunz, O., Klimeck, R., Wagner, W., and Jaeschke, M. 2007. The GERG-2004 Wide-Range Equation of State for Natural Gases and Other Mixtures. GERG TECHNICAL MONOGRAPH 15 (2007).

[12] Lei, X., Zhang, Q., Zhang, J., and Li, H. 2017. Experimental and Numerical Investigation of Convective Heat Transfer of Supercritical Carbon Dioxide at Low Mass Fluxes. Applied Sciences 7, 12, 1260.

[13] Liao, S. M. and Zhao, T. S. 2002. Measurements of Heat Transfer Coefficients From Supercritical Carbon Dioxide Flowing in Horizontal Mini/Micro Channels. Journal of Heat Transfer 124, 3, 413.

[14] Liu, Z.-B., He, Y.-L., Yang, Y.-F., and Fei, J.-Y. 2014. Experimental study on heat transfer and pressure drop of supercritical CO2 cooled in a large tube. Applied Thermal Engineering 70, 1, 307–315.

[15] McEligot, D. M. and Jackson, J. D. 2004. “Deterioration” criteria for convective heat transfer in gas flow through non-circular ducts. Nuclear Engineering and Design 232, 3, 327–333.

[16] Mendez, C. M. and Rochau, G. sCO2 Brayton Cycle: Roadmap to sCO2 Power Cycles NE Commercial Applications -SAND2018-6187. Sandia National Laboratories. SAND2018-6187. DOI=10.2172/1452896.

[17] Oh, H.-K. and Son, C.-H. 2010. New correlation to predict the heat transfer coefficient in-tube cooling of supercritical CO2 in horizontal macro-tubes. Experimental Thermal and Fluid Science 34, 8, 1230–1241.

[18] Pitla, S. S., Groll, E. A., and Ramadhyani, S. 2002. New correlation to predict the heat transfer coefficient during in-tube cooling of turbulent supercritical CO2. International Journal of Refrigeration 25, 7, 887–895.

[19] Riffat, S. B., Afonso, C. F., Oliveira, A. C., and Reay, D. A. 1997. Natural refrigerants for refrigeration and air-conditioning systems. Applied Thermal Engineering 17, 1, 33–42.

[20] S. Petukhov, B., A. Kurganov, V., and B. Ankudinov, V. 1983. Heat transfer and flow resistance in the turbulent pipe flow of a fluid with near-critical state parameters. Teplofizika Vysokikh Temperatur 21.

[21] Son, C.-H. and Park, S.-J. 2006. An experimental study on heat transfer and pressure drop characteristics of carbon dioxide during gas cooling process in a horizontal tube. International Journal of Refrigeration 29, 4, 539–546.

[22] Theologou, K., Mertz, R., Laurien, E., and Starflinger, J., Eds. 2019, 19-20. September. An Assessment of the criteria for the onset of heat transfer deterioration with supercritical CO_2 in vertical heated single circular tubes. DuEPublico: Duisburg-Essen Publications online, University of Duisburg-Essen, Germany.

[23] Vesovic, V., Wakeham, W.A., Olchowy, G.A., Sengers, J.V., Watson, J.T.R.,and Millat, J. 1990. The transport properties of carbon dioxide.

[24] W. Flaig, R. Mertz, and J. Starflinger, Eds. 2018, 30-31. August. Design, control procedure and start-up of the sCO_2 test facility SCARLETT.

[25] Yoon, S. H., Kim, J. H., Hwang, Y. W., Kim, M. S., Min, K., and Kim, Y. 2003. Heat transfer and pressure drop characteristics during the in-tube cooling process of carbon dioxide in the supercritical region. International Journal of Refrigeration 26, 8, 857–864.

DOI: 10.17185/duepublico/73957
URN: urn:nbn:de:hbz:464-20210330-103135-1